Smoyer et al., https://doi.org/10.1083/jcb.201607043

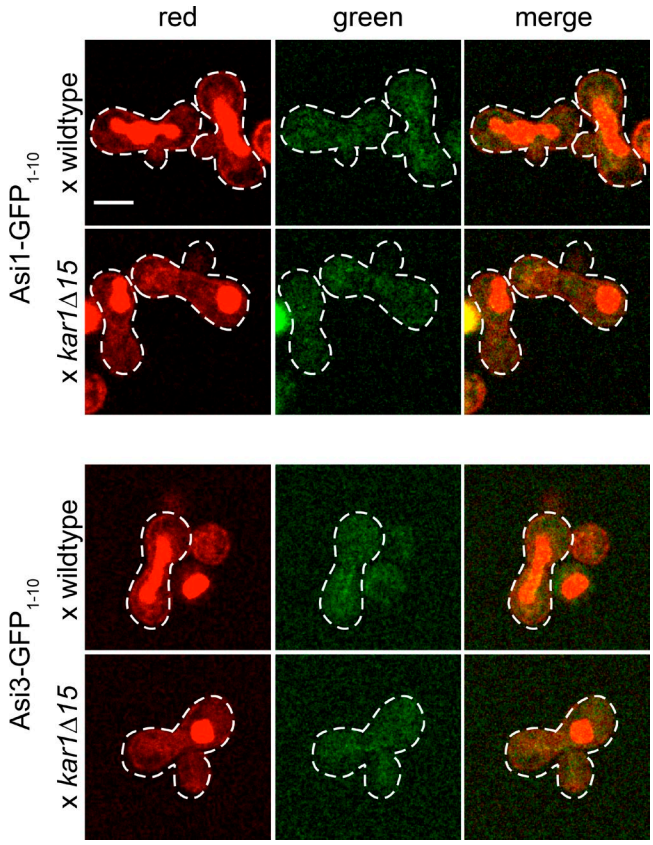

Figure S1. **Karyogamy-defective cells exhibit two distinct nuclei.** Haploid wild-type GFP_{11}-mCherry-Pus1 or *kar1Δ15* GFP_{11}-mCherry-Pus1 were mated to haploid cells containing a protein fused to $GFP_{1–10}$ and Sec61-mCherry for 2 h at 23°C. Images of wild-type cells show fused nuclei that contain signal at 488 nm; however, 488-nm signal was not observed in the binucleated *kar1Δ15* cells. Bar, 2 µm.

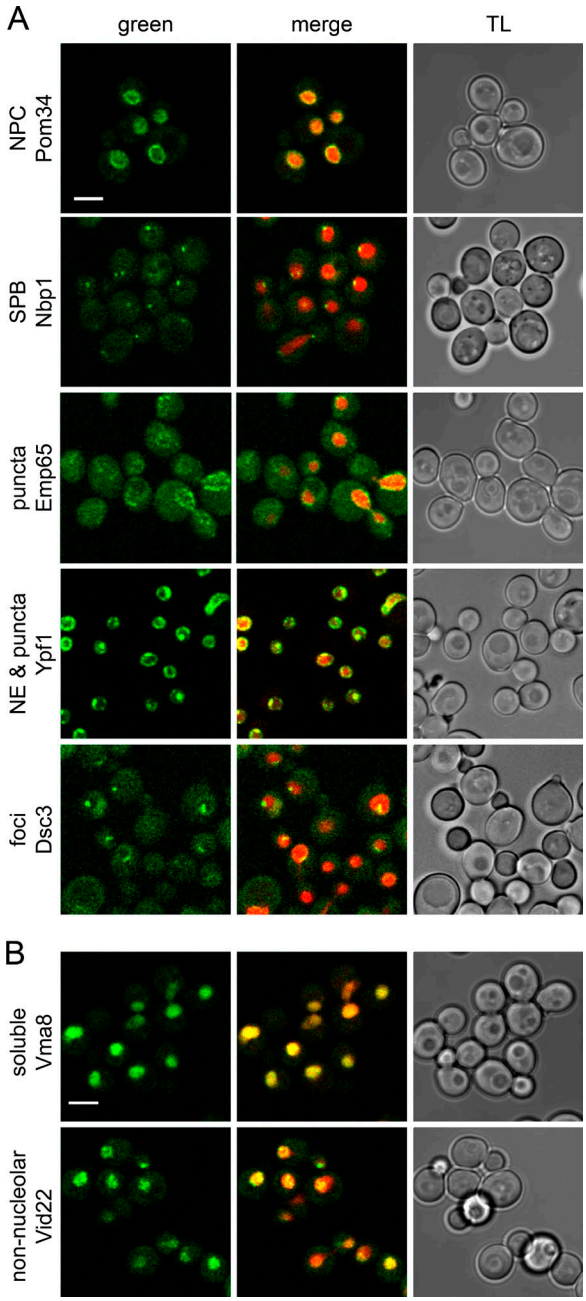

Figure S2. **Split-GFP illustrates other localization phenotypes.** (A) Representative images of subclasses of INM hits. Pom34: Similar to localization seen with GFP (Huh et al., 2003), we found that Pom152, Pom34, and Ndc1 localized to puncta at the NE that we presume are NPCs. Other soluble components of the NPC were not present in our screen, which is a major class of NE hits in the recent reanalysis of the yeast GFP collection (Chong et al., 2015). Nbp1: A single or double focus, depending on the cell-cycle stage, was observed for Nbp1, Ndc1, and Mps3. These represent the SPB, which is embedded in the NE throughout the yeast life cycle (Byers and Goetsch, 1975). Emp65: Sho1, Emp65, Fld1, Yip3, and Yop1 form puncta or foci at the INM, like some of their GFP counterparts (Huh et al., 2003; Friederichs et al., 2012). Similar to Emp65, the INM localization of Chs1, a plasma membrane protein involved in cytokinesis, also showed an uneven punctate pattern that was more visible in some cells. The paralogs Tda7 and YDL211c, both previously localized to the vacuole (Huh et al., 2003), form weak puncta at the INM. Ypf1: This ER protease showed a uniform pattern that also contained a few large foci. The paralogs Lag1 and Lac1 showed a similar pattern, particularly under DNA replication stress (Tkach et al., 2012). Dsc3: This protein showed a single NE-associated focus. Puncta outside the nucleus are caused by signal out of the focal plane shown or autofluorescence. (B) Images of nuclear hits, including a soluble protein present throughout the nucleoplasm (Vma8) and a nonnucleolar distribution (Vid22). Split-GFP is in green; GFP_{11}-mCherry-Pus1 is in red. A transmitted light image is also shown. Bars, 2 µm.

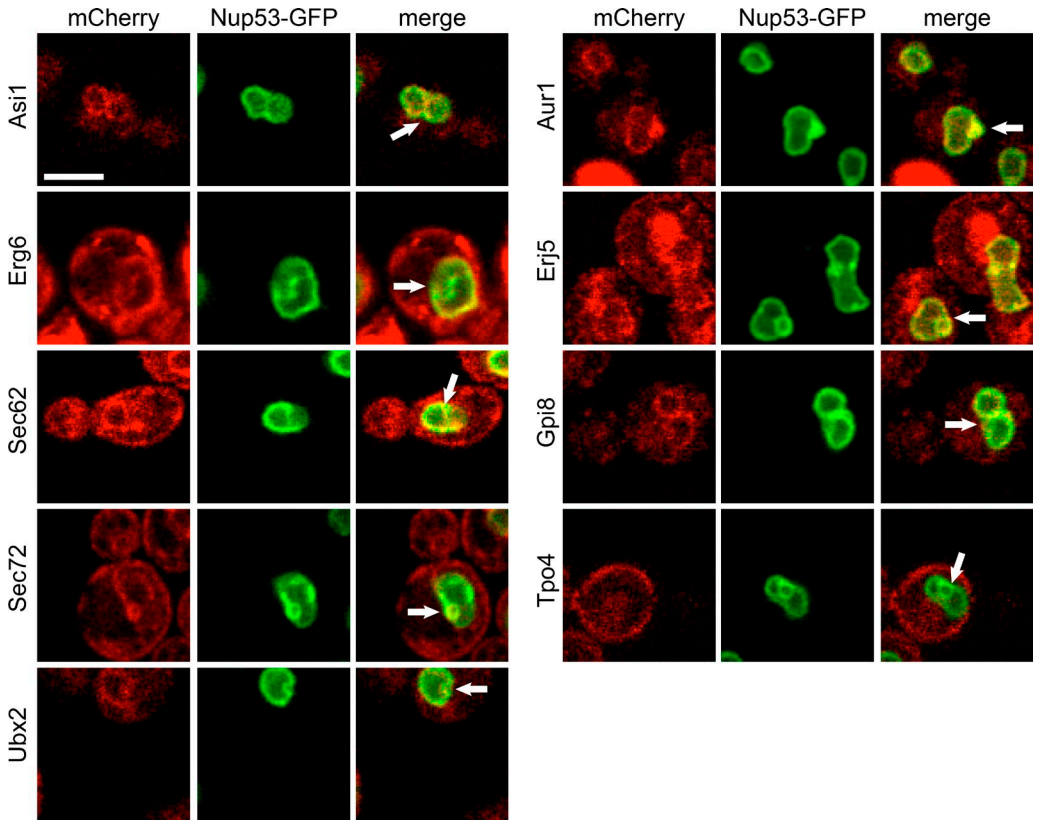

Figure S3. **Theta nuclei verify several low-scoring INM hits.** Single-plane images shown of theta nuclei induced by overexpression of Nup53-GFP (green) in 2% galactose for 5 h at 23°C. Arrows in merge images point to extra inner nuclear lamellae signal, where colocalization of the indicated mCherry-tagged protein was assayed. Example of the known Asi1 INM protein in a theta nucleus (top row), and theta nuclei verification of Erg6, Sec62, Sec72, Ubx2, Aur1 (low INM scores), Erj5 (nonscore), and Gpi8 (high INM score). Sec62, Ubx2, Erj5, and Gpi8 were also verified by immuno-EM (see Fig. 5). Tpo4 was a low-scoring hit that did not verify as an INM hit via the theta nuclei assay (bottom right). Bar, 2 µm.

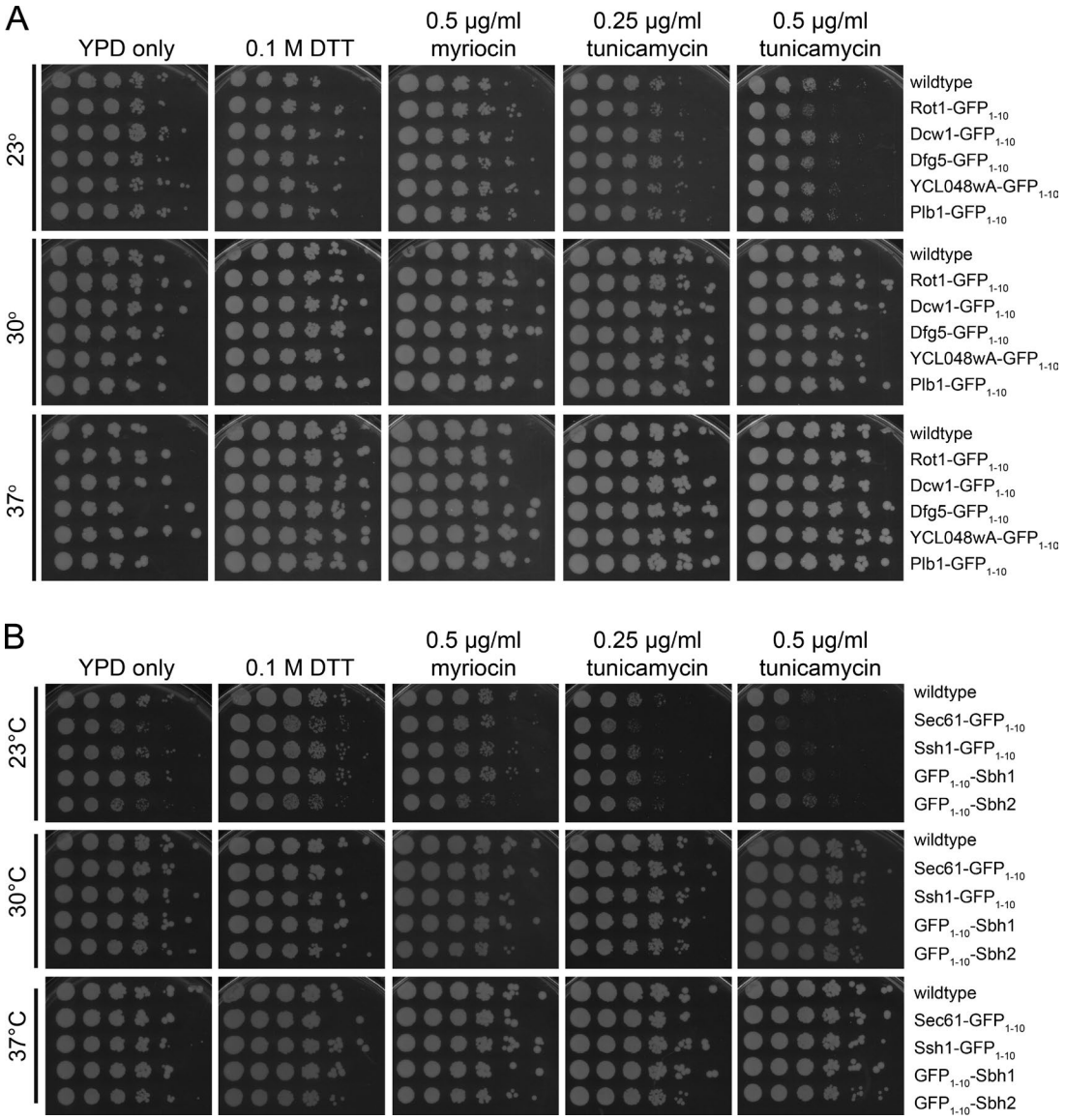

Figure S4. **Growth of selected split-GFP tagged ER–INM hits.** (A) Fivefold serial dilutions of strains containing the indicated C-terminally $GFP_{1–10}$ tagged GPI-anchored proteins were grown on YPD alone or with 2.5 mM DTT, 0.5 µg/ml myriocin, or 0.25–0.5 µg/ml tunicamycin at 23°C, 30°C, and 37°C for 3 d. *ROT1* is an essential gene, the other four are nonessential in yeast. All were hits in our C-terminal screen. (B) Fivefold serial dilutions of strains containing endogenously expressed Sec61-$GFP_{1–10}$, Ssh1-$GFP_{1–10}$, $GFP_{1–10}$-Sbh1, and $GFP_{1–10}$-Sbh2 were grown on YPD alone or with 2.5 mM DTT, 0.5 µg/ml myriocin, or 0.25–0.5 µg/ml tunicamycin at 23°C, 30°C, and 37°C for 3 d. Sec61-$GFP_{1–10}$ exhibited a mild growth defect on tunicamycin at 23°C.

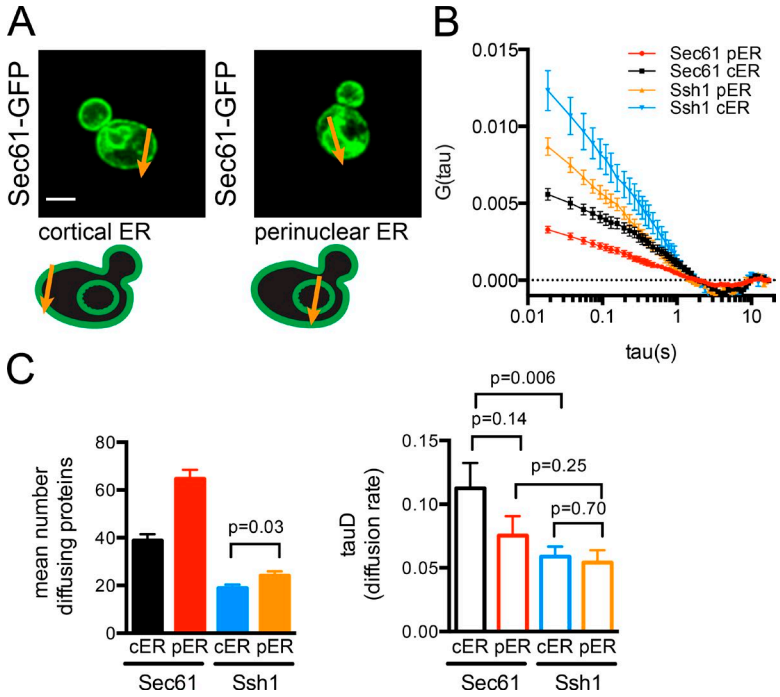

Figure S5. **FCS of Sec61 and Ssh1 reveals different characteristics in the cortical and perinuclear ER.** (A) Focal volumes defined by arrows to include the perinuclear and cortical ER for Sec61-GFP were used to collect linescan data and perform correlation analysis. (B) Mean autocorrelation curves of Sec61 and Ssh1 based on GFP images at the perinuclear (n = 28, both Sec61 and Ssh1) and cortical ER (n = 19, Sec61; n = 28, Sbh1) are shown. (C) For each sample, the diffusion rate and number of diffusing molecules were determined, and mean values are plotted. Bar, 2 µm. Error bars indicate SEM. P-values were calculated using the Student's t test. All values were highly statistically significant ($P < 0.01$) unless noted otherwise.

Table S1. **FCS data for ER translocon proteins**

Protein/membrane	Diffusion	SEM Diffusion	n^a	SEM	Fraction INM	Propagated error
Sec61 INM	0.209	0.033	20.004	1.688	0.185	0.019
Sec61 NE	0.096	0.024	108.049	6.280		
Sec61 cortical ER	0.064	0.013	64.817	4.474		
Sec62 INM	0.636	0.164	4.339	0.390	0.184	0.022
Sec62 NE	0.374	0.050	23.553	1.804		
Sec62 cortical ER	0.220	0.058	18.204	1.831		
Sec63 INM	0.162	1.891	7.404	1.281	0.358	0.072
Sec63 NE	0.140	0.176	20.676	1.995		
Sec63 cortical ER	0.155	0.024	14.492	0.974		
Sec66 INM	0.481	0.171	7.272	0.853	0.381	0.053
Sec66 NE	0.193	0.399	19.076	1.363		
Sec66 cortical ER	0.223	0.036	18.729	1.370		
Sec72 INM	0.288	0.129	7.355	0.700	0.290	0.034
Sec72 NE	0.183	0.030	25.367	1.715		
Sec72 cortical ER	0.157	0.031	20.144	1.650		
Ssh1 INM	0.051	0.009	16.602	1.113	0.412	0.042
Ssh1 NE	0.133	0.028	40.284	3.055		
Ssh1 cortical ER	0.122	0.018	31.602	2.305		

Diffusion rate reported as micrometer squared per second. Linescanning FCS was performed on cortical and perinuclear ER using GFP-tagged proteins. $GFP_{1–10}$ was used to collect INM data.
[a]Mean number of molecules diffusing through focus.

Table S2. **Yeast strains used in this study**

Figure	Strain number	Relevant genotype
1 (B and D), 2, S1	SLJ7859	SLJ1838 p*NOP1pr-GFP11-mCherry-PUS1-LEU2* (pSJ1321)
1 B	SLJ8349	SLJ1838 *asi1::ASI1-GFP1-10-URA3MX*
1 B	SLJ7859	SLJ1838 *asi1::ASI1-GFP1-10-URA3MX pNOP1pr-GFP11-mCherry-PUS1-LEU2* (pSJ1321)
1 D, 2	SLJ7465	SLJ1838 p*NOP1pr-GFP11-mCherry-SCS2TM-LEU2* (pSJ1568)
1 D, 2	SLJ8344	SLJ1838 p*NOP1pr-mCherry-SCS2TM-GFP11-LEU2* (pSJ1602)
1 D, 2	SLJ1838	SLJ1838 p*NOP1pr-GFP11-mCherry-HXK1-LEU2* (pSJ1996)
1 D	SLJ11810	BY4741 p*NOP1pr-GFP1-10-SCS2TM* (pSJ2039) p*NOP1pr-GFP11-mCherry-PUS1-LEU2* (pSJ1321)
1 D	SLJ11812	BY4741 p*NOP1pr-GFP1-10-SCS2TM* (pSJ2039) p*NOP1pr-GFP11-mCherry-SCS2TM-LEU2* (pSJ1568)
1 D	SLJ11813	BY4741 p*NOP1pr-GFP1-10-SCS2TM* (pSJ2039) p*NOP1pr-mCherry-SCS2TM-GFP11-LEU2* (pSJ1602)
1 D	SLJ11814	BY4741 p*NOP1pr-GFP1-10-SCS2TM* (pSJ2039) p*NOP1pr-GFP11-mCherry-HXK1-LEU2* (pSJ1996)
2, 3 B, 3 C, 6 (A and B), 7 (B, C, and E), 8 B, S2 (A and B), S4 (A and B)	C-terminal split-GFP library	SLJ7859 plus PCR product from pSJ1256
2, 6B	N-terminal split-GFP library	SLJ7859 plus PCR product from pSJ1643 or pSJ1726
3C	SLJ9739*	*sec66Δ::HYGMX sec72::SEC72-GFP1-10-URA3MX pNOP1pr-GFP11-mCherry-PUS1-LEU2* (pSJ1321)
5 (A and B), 6 B, 7 (B, C, and E), S5 A	Yeast GFP collection	*MATa his3Δ1 leu2Δ0 ura3Δ0 met15Δ0 yfg::YFG-HIS3MX*
5C	SLJ10338	W303 *sec63::SEC63-mCherry-KANMX ura3::GAL-NUP53-GFP-URA3*
5C	SLJ11379	W303 *sec66:SEC66-mCherry-KANMX ura3::GAL-NUP53-GFP-URA3*
5C	SLJ11434	W303 *gpi17::GPI17-mCherry-KANMX ura3::GAL-NUP53-GFP-URA3*
5C	SLJ11384	W303 *get1::GET1-mCherry-KANMX ura3::GAL-NUP53-GFP-URA3*
5C	SLJ11408	W303 *yop1::YOP1-mCherry-KANMX ura3::GAL-NUP53-GFP-URA3*
5C	SLJ11383	W303 *vph1::VPH1-mCherry-KANMX ura3::GAL-NUP53-GFP-URA3*
7E	SLJ9809	SLJ7465 *sec62::SEC62-GFP1-10-URA3MX*
8C	SLJ10163	*MATa/MATα can1Δ::STE2pr-SpHIS5/CAN1 lyp1Δ/lyp1Δ his3Δ1/ his3Δ1 leu2Δ0/ leu2Δ0 ura3Δ0/ ura3Δ0 met15Δ0/met15Δ0 LYS2/LYS2 trp1Δ::HYGMX/TRP1*
8 (C and E), S4 B	SLJ10954	SLJ7859 *sbh1::LoxP-GFP1-10-SBH1*
8 C, S4 B	SLJ11376	SLJ7859 *sbh2::LoxP-GFP1-10-SBH2*
8E	SLJ10956*	*sbh2Δ::HYGMX sbh1::LoxP-GFP1-10-SBH1*
8F	SLJ10954	SLJ7465 *sbh1::LoxP-GFP1-10-SBH1*
9B	SLJ11340**	*sbh2::LoxP-GFP-SBH2 sec61::SEC61-mCherry-HYGMX*
9B	SLJ11010*	*sbh2::LoxP-GFP1-10-SBH2 sec61::SEC61-mCherry-HYGMX*
S1	SLJ7859kar1Δ15	SLJ1838 *kar1Δ15 pNOP1pr-GFP11-mCherry-PUS1-LEU2* (pSJ1321)
S1	SLJ11210*	*sec61::SEC61-mCherry-KANMX asi3::ASI3-GFP1-10-URA3MX*
S1	SLJ11211*	*sec61::SEC61-mCherry-KANMX asi1::ASI1-GFP1-10-URA3MX*
S3	SLJ11423	W303 *asi1::ASI1-mCherry-KANMX ura3::GAL-NUP53-GFP-URA3*
S3	SLJ11381	W303 *erg6::ERG6-mCherry-KANMX ura3::GAL-NUP53-GFP-URA3*
S3	SLJ11410	W303 *sec62::SEC62-mCherry-KANMX ura3::GAL-NUP53-GFP-URA3*
S3	SLJ11377	W303 *sec72::SEC72-mCherry-KANMX ura3::GAL-NUP53-GFP-URA3 LYS+ Matα*
S3	SLJ11378	W303 *ubx2::UBX2-mCherry-KANMX ura3::GAL-NUP53-GFP-URA3*
S3	SLJ11444	W303 *aur1::AUR1-mCherry-KANMX ura3::GAL-NUP53-GFP-URA3*
S3	SLJ11443	W303 *erj5::ERJ5-mCherry-KANMX ura3::GAL-NUP53-GFP-URA3*
S3	SLJ11433	W303 *gpi8::GPI8-mCherry-KANMX ura3::GAL-NUP53-GFP-URA3*
S3	SLJ11478	W303 *tpo4::TPO4-mCherry-KANMX ura3::GAL-NUP53-GFP-URA3*
Base strain	SLJ1838	*MATα can1Δ::STE2pr-SpHIS5 lyp1Δ his3Δ1 leu2Δ0 ura3Δ0 met15Δ0 LYS2*
Base strain	BY4741	*MATa his3Δ1 leu2Δ0 ura3Δ0 met15Δ0 LYS2*
Base strain	W303	*MATa bar1 leu2-3,112 his3-11,15 lys2 TRP1 ADE2*
*Generated via cross	BY4741 × SLJ7859	*MATa can1Δ::STE2pr-SpHIS5 lyp1Δ his3Δ1 leu2Δ0 ura3Δ0 met15Δ0 LYS2 pNOP1pr-GFP11-mCherry-PUS1-LEU2* (pSJ1321)
**Generated via cross/ plasmid swap	BY4741 × SLJ7859	*MATa can1Δ::STE2pr-SpHIS5 lyp1Δ his3Δ1 leu2Δ0 ura3Δ0 met15Δ0 LYS2 pNOP1pr-GFP11-PUS1-LEU2* (pSJ1679)

Provided online are three Excel tables. Table S3 shows the results of split-GFP1–10 screen. Table S4 shows proteins that access the yeast INM based onthe split-GFP1–10 screen. For predicted single-pass transmembrane proteins (by Phobius and TMHMM), molecular masses of start and end (before and after transmembrane, respectively) are estimated. Table S5 shows contribution of proteins with known C-terminal motifs to our library. It also includes a list of proteins that contain a C-terminal GPI-anchor, tail-anchored, or HDEL or CaaX motifs. Genes included in our library are annotated, as well as the results of screening, when applicable.

References

Byers, B., and L. Goetsch. 1975. Behavior of spindles and spindle plaques in the cell cycle and conjugation of *Saccharomyces cerevisiae. J. Bacteriol.* 124:511–523.

Chong, Y.T., J.L. Koh, H. Friesen, S.K. Duffy, M.J. Cox, A. Moses, J. Moffat, C. Boone, and B.J. Andrews. 2015. Yeast proteome dynamics from single cell imaging and automated analysis. *Cell.* 161:1413–1424. http://dx.doi.org/10.1016/j.cell.2015.04.051

Friederichs, J.M., J.M. Gardner, C.J. Smoyer, C.R. Whetstine, M. Gogol, B.D. Slaughter, and S.L. Jaspersen. 2012. Genetic analysis of Mps3 SUN domain mutants in *Saccharomyces cerevisiae* reveals an interaction with the SUN-like protein Slp1. *G3 (Bethesda).* 2:1703–1718. http://dx.doi.org/10.1534/g3.112.004614

Huh, W.K., J.V. Falvo, L.C. Gerke, A.S. Carroll, R.W. Howson, J.S. Weissman, and E.K. O'Shea. 2003. Global analysis of protein localization in budding yeast. *Nature.* 425:686–691. http://dx.doi.org/10.1038/nature02026

Tkach, J.M., A. Yimit, A.Y. Lee, M. Riffle, M. Costanzo, D. Jaschob, J.A. Hendry, J. Ou, J. Moffat, C. Boone, et al. 2012. Dissecting DNA damage response pathways by analysing protein localization and abundance changes during DNA replication stress. *Nat. Cell Biol.* 14:966–976. http://dx.doi.org/10.1038/ncb2549